

# We are IntechOpen, the world's leading publisher of Open Access books Built by scientists, for scientists

6,900

Open access books available

186,000

International authors and editors

200M

Downloads

Our authors are among the

154

Countries delivered to

TOP 1%

most cited scientists

12.2%

Contributors from top 500 universities



WEB OF SCIENCE™

Selection of our books indexed in the Book Citation Index  
in Web of Science™ Core Collection (BKCI)

Interested in publishing with us?  
Contact [book.department@intechopen.com](mailto:book.department@intechopen.com)

Numbers displayed above are based on latest data collected.  
For more information visit [www.intechopen.com](http://www.intechopen.com)



---

# Thermomechanical Treatments for Ni-Ti Alloys

---

F.M. Braz Fernandes, K.K. Mahesh and Anderson dos Santos Paula

Additional information is available at the end of the chapter

<http://dx.doi.org/10.5772/56087>

---

## 1. Introduction

Thermomechanical treatments for shape memory alloys (SMA) are found to be one of the more economical, simpler, and efficient methods adopted for manipulating the transformation properties. The stability of phase transformation has been found to depend upon the thermomechanical treatments, such as hot- or cold-working, heat-treatment and thermal cycling. It has perhaps more important and wide reaching ramifications than many of the other stages in the fabrication of components and structures.

During the stages of preparation of SMA, hot working is adopted as one of processes in the form of rolling or drawing to incorporate the shape memory effect (SME). Such alloys can be directly employed for the applications. However, most of the times, the ingots are finally cold worked in the form of rolling or drawing before delivering to the application purpose. This allows the application engineers to subject the alloys to appropriate thermal/mechanical treatment in order to obtain the SMA with desired phase transformation properties. Hence, a sequence of cold work followed by heat treatment is considered to be a productive method to tailor the SME and superelasticity (SE).

In order to emphasize the various methods of thermal, mechanical, and thermomechanical treatments, the Chapter is divided into the following Sections and Sub-sections.

- i. Cold working
- ii. Cold working followed by heat treatments
- iii. Effect of cooling rate during heat treatments
- iv. Hot working
- v. Thermal cycling
- vi. Severe plastic deformation
  - a. High-pressure torsion (HPT)
  - b. Equal channel angular pressing (ECAP)
- vii. Concluding remarks

## 2. Cold working

Cold working can induce dislocations and vacancies in the Nickel-Titanium (Ni-Ti) alloys. It is suggested that the possible mechanisms for the martensite stabilization in the Equiatomic Ni-Ti alloys come from deformed structures and deformation induced dislocations/vacancies. Thermomechanical treatments of Ni-Ti SMA are important for the optimization of the mechanical properties and phase transformation characteristics. An important characteristic in the Ni-Ti SMA is the stability on direct and reverse transformations, related to the sequence and transformation temperatures, and thermal hysteresis [1-5]. The transformation temperatures in Ni-Ti SMA have been shown to be related to the presence of lattice defects introduced by cold working [6, 7]. Wu *et al.*, (1996) showed that the defects induced during cold working have the effect of suppressing the martensitic transformation and promoting the R-phase transformation [8]. The residual internal stress induced by cold-working defects is considered to be responsible for the R-phase transformation [9]. The deformation mechanisms and morphologies in polycrystalline martensitic CuZnAl alloy have been examined by Adachi and Perkins [10]. They observed that a variety of deformation morphologies, including variant-variant coalesce, stress-induced martensite to martensite transformation, injection of foreign variants to plate groups, and internal twinning and slip, are all exhibited simultaneously in moderately cold-worked specimens.

Ni-Ti alloys have a wider application in the form of wires. Therefore, an understanding of the wire drawing properties is important. Thin oxide film with a smooth surface on TiNi wires can be used as a lubricant during the drawing process. However, thick oxide films which have cracks and spalling on the surface can be detrimental to the drawing surface and depress the shape memory effect and pseudoelasticity of TiNi SMA. MoS<sub>2</sub> is an effective lubricant for wire drawing of TiNi SMA [8]. Also, cold rolling has been one of the widely adopted processing techniques in order to obtain Ni-Ti alloy in the sheet form. In a study of the cold-rolled equiatomic TiNi alloy, it was found that the same phenomena of martensite stabilization appear, as reported in Cu-based shape memory alloys [9, 10]. It is well known that the martensite in the Ti<sub>50</sub>Ni<sub>50</sub> alloy has 24 variants [11]. The variants will accommodate each other under thermal or mechanical stress. It is reasonable to suggest that the stress exerted by cold rolling causes the variants to accommodate, i.e., the stress forces the preferred orientated variants to accommodate the deformation strain in the favorable stress direction. An intensive study of the microstructure of the deformed martensite shows, in addition to the deformed martensite plates, a large number of dislocations and vacancies can also be induced during the cold rolling. These deformation-induced dislocations and vacancies have an important effect on the martensitic stabilization [9].

In Fig. 1, DSC thermograms of the Ni-Ti alloy plate subjected to 40% cold working are shown. When the cold worked specimen is heated from RT up to around 300°C, no phase transformation is observed and on the further heating, a broad upward peak appears around 350°C corresponding to recrystallization process. However, on cooling to RT, a clear exothermic peak appears around 75°C and that is attributed to A→M phase transformation. While heating again from RT, the DSC thermogram shows an endothermic peak around

85 °C corresponding to  $M \rightarrow A$  phase transformation and while cooling the reverse phase transformation,  $A \rightarrow M$ , is observed.

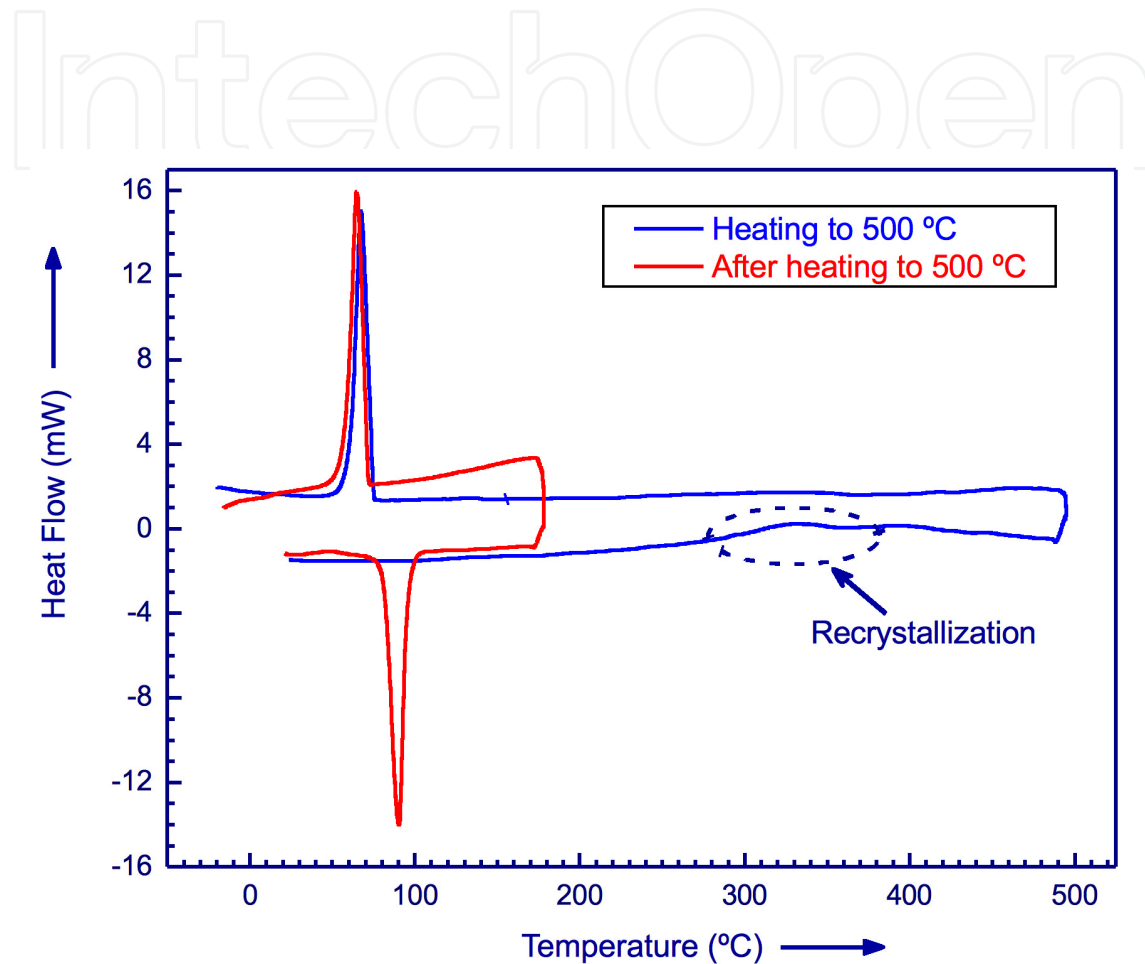


**Figure 1.** DSC thermograms of the Ni-Ti SMA plate initially cold worked up to 40% and heated to 500°C (in blue), and after (in red).

In Fig. 2, 3-d representation of the XRD profiles obtained at different temperatures from RT to 400°C for the 40% cold worked Ni-Ti specimen is shown. XRD spectra obtained at RT show the peaks corresponding to B19' structure, which are broad and with low intensity. As the temperature is increased, the peak corresponding to B2 structure starts to emerge around 190 °C and on further heating, the intensity of the peak increases. Broad and low intensity peaks are due to the deformation induced dislocations and vacancies which suppresses the martensitic transformation [12-14].

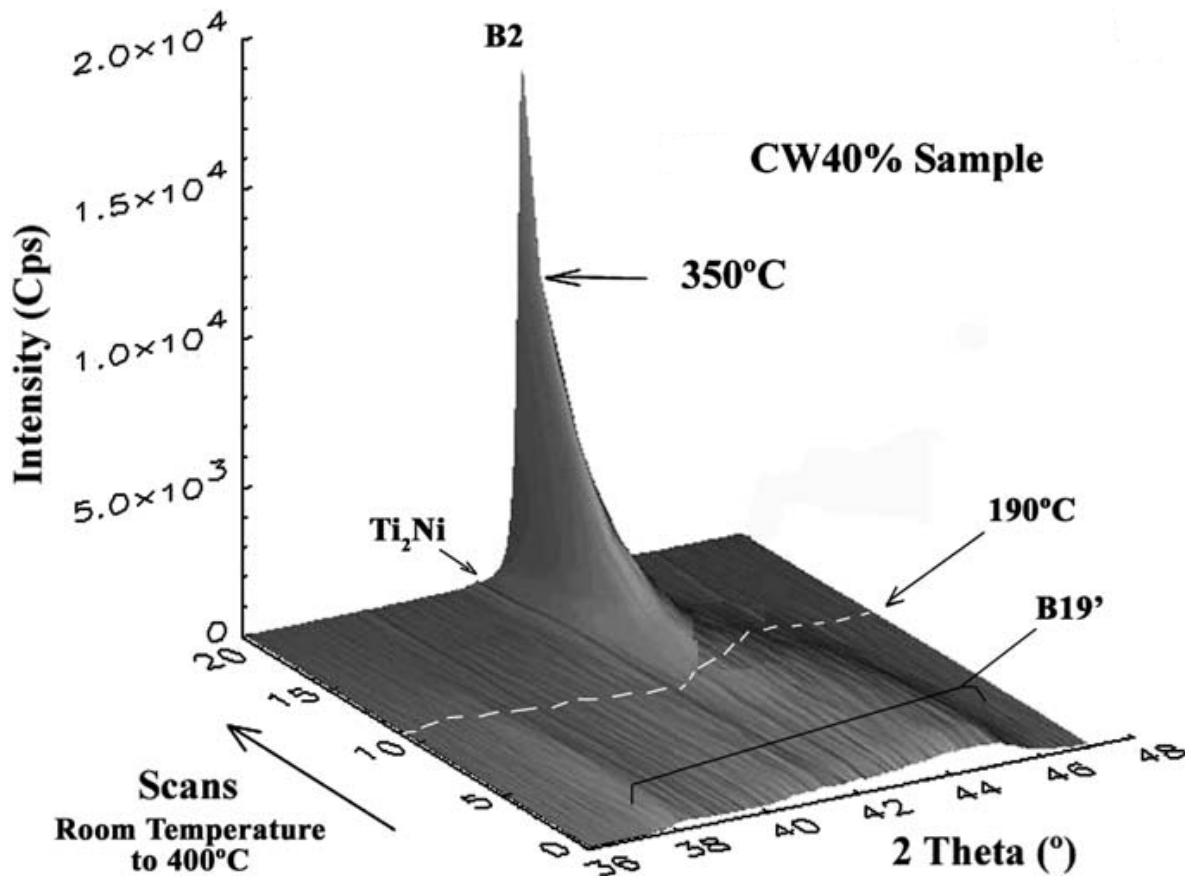


**Figure 2.** 3-d representation of the XRD profiles obtained at different temperatures from RT to 400°C for the 40% cold worked Ni-Ti specimen.

### 3. Cold working followed by heat treatments

Heat treatment for metals and alloys has been proved to be an effective and economical process in order to maneuver their properties. Various factors, such as the HTT, annealing time and cooling rate after annealing have their own effects on the final state of the metal/alloy. In the above sub-section, it is mentioned that the defects induced during cold working have the effect of suppressing the martensitic transformation [8]. On the contrary, there is a possibility that a reverse phenomenon (restoration) would occur in a rather enhanced manner upon annealing through thermal activation processes of point defects. The migration of vacancies and interstitials could facilitate promotion of the martensitic transformation [15]. In this sub-section, the dependence of heat-treatment on the composition and thermal/mechanical history of the alloys has been explained. Heat-treatment plays a crucial role in fixing  $M_s$ . The detection of R-phase is found to be critical with the positioning of  $M_s$  in relation to  $R_s$ . If  $M_s$  is above  $R_s$ , R-phase is found to be masked by the martensite phase. Earlier, from electrical resistivity measurements, it was shown that while cooling from austenite phase, if R-phase exists, it preceded the martensite phase and it was regarded as the pre-martensitic phase [16]. However, later it was shown that both phases coexist at the same temperature, and it has been confirmed by the DSC study on the

phase transformation in the 40% cold worked, near equi-atomic NiTi alloy subjected to water quenching from 400°C [17].

Phase transformations associated with SME in Ni-Ti alloys can be one-stage,  $B19' \leftrightarrow B2$ , two-stage including an intermediate R-phase stage, or multiple-stage depending on the thermal and/or mechanical history of the alloy. In a recent report, it has been highlighted the effect of (i) deformation by cold-rolling (from 10% to 40% thickness reduction) and (ii) final annealing on the transformation characteristics of a Ti-rich NiTi shape memory alloy. For this purpose, one set of samples initially heat treated at 500 °C followed by cold-rolling (10–40% thickness reduction) has been further heat treated at various temperatures between 400 and 800 °C. Phase transformations were studied using differential scanning calorimetry, electrical resistivity measurements and in situ X-ray diffraction. A specific pattern of transformation sequences is found as a result of combination of the competing effects due to mechanical-working and annealing [18].

Fig. 3 (a & b) show the Differential Scanning Calorimeter (DSC) and Electrical Resistivity (ER) curves for (i) as-received (AR), (ii) annealed at 500°C (HT500) and (iii) annealed at 500 °C/cold-rolled to 30%/annealed at 500°C (TMTCR30HT500) samples. For the AR sample, both in the case of DSC & ER techniques, multiple-step ( $B2 \leftrightarrow R$ ,  $B2 \leftrightarrow B19'$ ,  $R \leftrightarrow B19'$ , while heating and cooling) phase transformations are observed. For the HT500 sample, in both

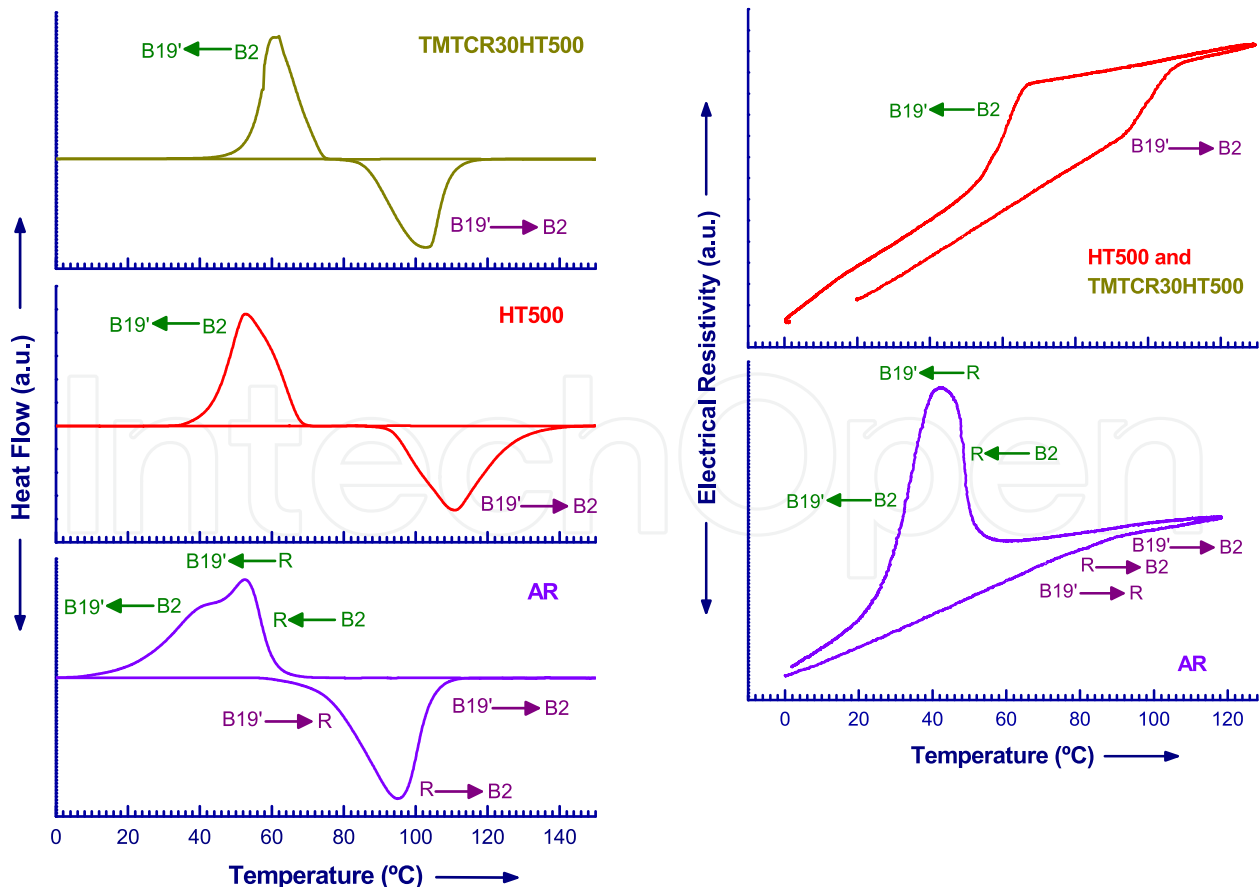


**Figure 3.** (a) DSC and (b) ER curves for AR, HT500 and TMTCR30HT500 samples

techniques, during heating and cooling, one-step ( $B19' \leftrightarrow B2$ ) phase transformation is found to be present. Further, in the case of TMTCR30HT500 sample, one-step ( $B19' \leftrightarrow B2$ ) phase transformation is detected. During heating (for AR samples), a small kink in the DSC and a small hump in ER plots around 60 °C show the presence of R-phase associated to multiple-step, ( $B19' \leftrightarrow R$ ,  $B19' \leftrightarrow B2$ ,  $R \leftrightarrow B2$ ), phase transformation.

The effects of various heat treatment temperatures (HTT) on samples after being cold-rolled to different extents (10 to 40% thickness reduction) are presented in Fig. 4. All the samples were annealed at 500 °C before cold-rolling. Figs. 4 (a to d) show the transformation temperatures ( $A_f$ ,  $A_s$ ,  $R_{fh}$ ,  $R_{sh}$ ,  $R_{sc}$ ,  $R_{fc}$ ,  $M_s$  and  $M_f$ , obtained from DSC thermograms) as a function of HTT, for the samples annealed after being cold worked up to 10%, 20%, 30% and 40%, respectively. "A", "R" and "M" are the austenite, rhombohedral, and martensite phases; suffixes "s" and "f" are the start (1%) and finish (99%) transformation temperatures; and "c" and "h" refer to cooling and heating, respectively.

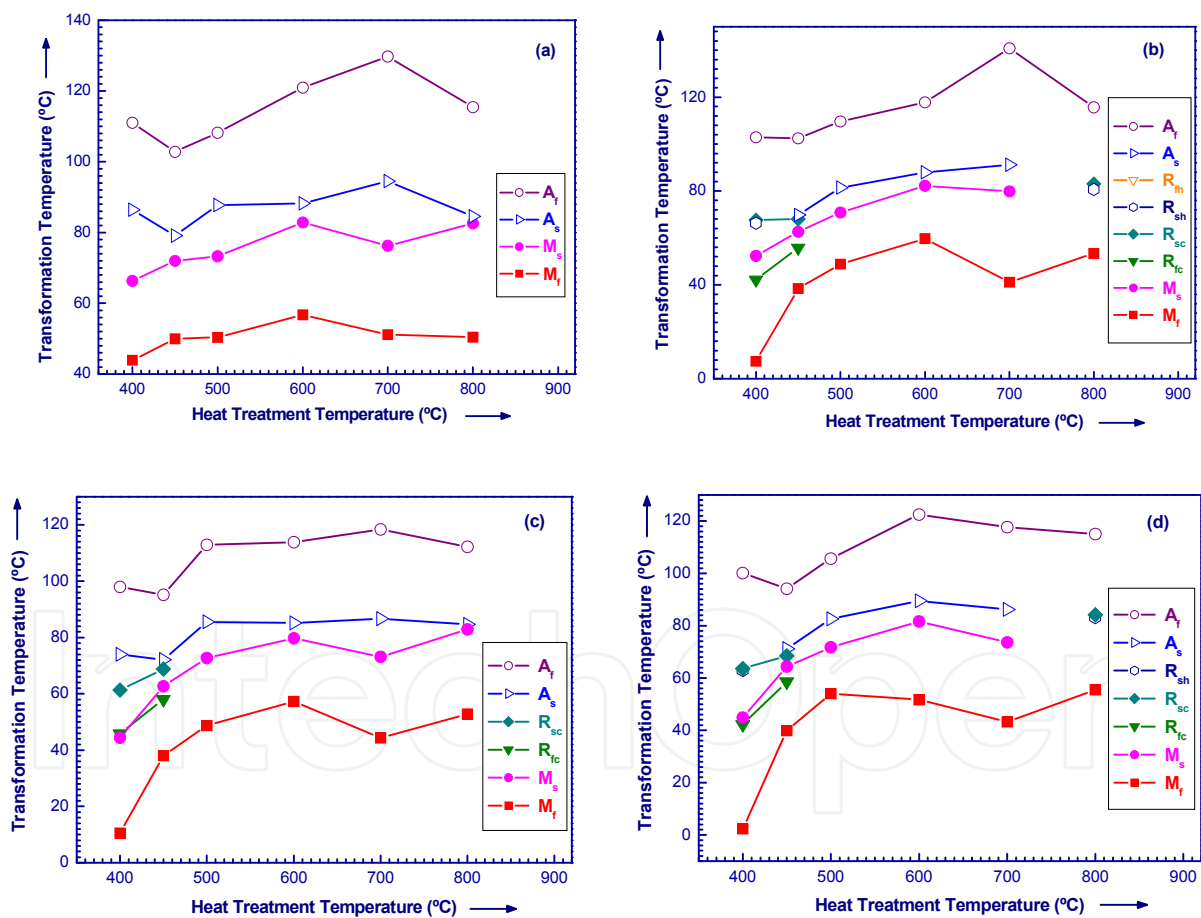


**Figure 4.** Transformation temperatures of (a) TMTCR10%, (b) TMTCR20%, (c) TMTCR30%, and (d) TMTCR40%

In Fig. 4(a), for the 10% cold worked samples, as the final annealing temperature is increased,  $M_s$  and  $M_f$  are found to increase gradually up to 600 °C followed by a slight drop up to 800 °C.  $A_s$  and  $A_f$  are found to decrease as the final annealing temperature is increased

from 400 to 500 °C. Further increase up to 700 °C shows gradual increase followed by a decrease for the final annealing temperature of 800 °C.

In Fig. 4(b), it is observed that for the 20% cold worked samples, there is R-phase formation while cooling ( $R_{sc}$ ,  $R_{fc}$ ) and while heating ( $R_{sh}$ ). As the final annealing temperature is increased,  $R_{sc}$  and  $R_{fc}$  are found to increase till 500 °C. For higher final annealing temperatures, the R-phase formation is no longer detected.  $M_s$  and  $M_f$  increase with increasing final annealing temperature until it reaches 600 °C, followed by a slight decrease when the sample is heat treated at 700 °C. For the final annealing at 800 °C,  $M_s$  is not possible to be determined, but  $M_f$  increases slightly.  $A_s$  is found to increase with increasing final annealing temperature up to 700 °C along with  $A_f$ . For the final annealing temperature of 800 °C,  $A_s$  was not possible to be determined and  $A_f$  decreases. For this same treatment (800 °C), the R-phase formation is once again detected during cooling and heating.

In the case of samples 30% cold worked, as shown in Fig. 4(c); the R-phase is only present during cooling for final annealing temperatures up to 500 °C ( $R_{sc}$  and  $R_{fc}$  increase with increasing final annealing temperature).  $M_s$  and  $M_f$  increase for increasing final annealing temperature up to 600 °C, slightly decrease for 700 °C and then slightly increase for 800 °C.  $A_s$  and  $A_f$  slightly decrease from 400 to 500 °C and then increase and stabilize after 500 °C.

In Fig. 4(d), it is observed that for the samples 40% cold worked and heat treatment there is R-phase formation only during cooling for the final annealing temperature up to 500 °C. ( $R_{sc}$  and  $R_{fc}$  are found to increase with increasing annealing temperature).  $M_s$  and  $M_f$  increase with increasing final annealing temperature till 600 °C. For the final annealing temperature of 800 °C,  $M_s$  and  $A_s$  were not possible to be determined. For the final annealing temperature of 800 °C, the R-phase formation is once again detected.

The absence of the R-phase formation in the sample annealed at 500 °C (not cold-rolled), may be explained by the annealing out of the structural defects and generation of the strain free crystals [19]. The same result is observed for the sample that has been cold-rolled to 10% (very close to the maximum recoverable strain of this class of alloys). With increasing extent of cold-work deformation, the R-phase deformation is only detectable for final annealing temperatures below 500 °C or at 800 °C. The final annealing temperature above 500 °C induces a recrystallization of the marformed matrix that makes the single-step transformation  $B2 \leftrightarrow B19'$  more favorable [14, 20, 21]. This transformation may be initiated at the coherent interfaces of the very narrow precipitates  $Ti_2Ni$ . For the highest final annealing temperature (800 °C) the R-phase formation is once again present and this may be associated to the coalescence of the  $Ti_2Ni$  precipitates, making the B2 /  $Ti_2Ni$  interfaces incoherent [22, 23]. When the DSC and ER results in Figs. 1 and 2 are compared, it is apt to mention that when there is overlap of the phases transformation, ER technique is in a better position to reveal the presence of distinct phases.

Table 1 summarizes the transformation sequences of the samples after the thermomechanical treatments. For the samples cold worked to 10% and subsequently heat treated up to 700 °C, the transformation sequence is found to be clearly one-step ( $B19' \leftrightarrow B2$ ). On the other hand, no matter the thickness reduction by cold-rolling, when the final

annealing temperature is between 500 °C and 700 °C, the transformation is also clearly one-step ( $B19' \leftrightarrow B2$ ). The two-steps phase transformation while cooling is only observed for the samples cold-rolled to 30 and 40% and for the final annealing temperatures of 400 °C. The multiple-steps phase transformation (with overlap) is only observed in two situations: (i) for the final annealing temperature of 800 °C, no matter the cold-work reduction, both while cooling and heating, and (ii) for the samples cold-worked to 20 to 40%, where the final annealing temperature was 500 °C or below.

HTT (°C)	Reduction by Cold Rolling			
	10%	20%	30%	40%
400	+ / +	⊕ / ∅	++ / +	++ / ∅
450	+ / +	⊕ / ∅	⊕ / ∅	⊕ / ∅
500	+ / +	+ / +	+ / +	+ / +
600	+ / +	+ / +	+ / +	+ / +
700	+ / +	+ / +	+ / +	+ / +
800	∅ / ∅	∅ / ∅	∅ / ∅	∅ / ∅

On Cooling / On Heating: + one-step; ++ two-steps;

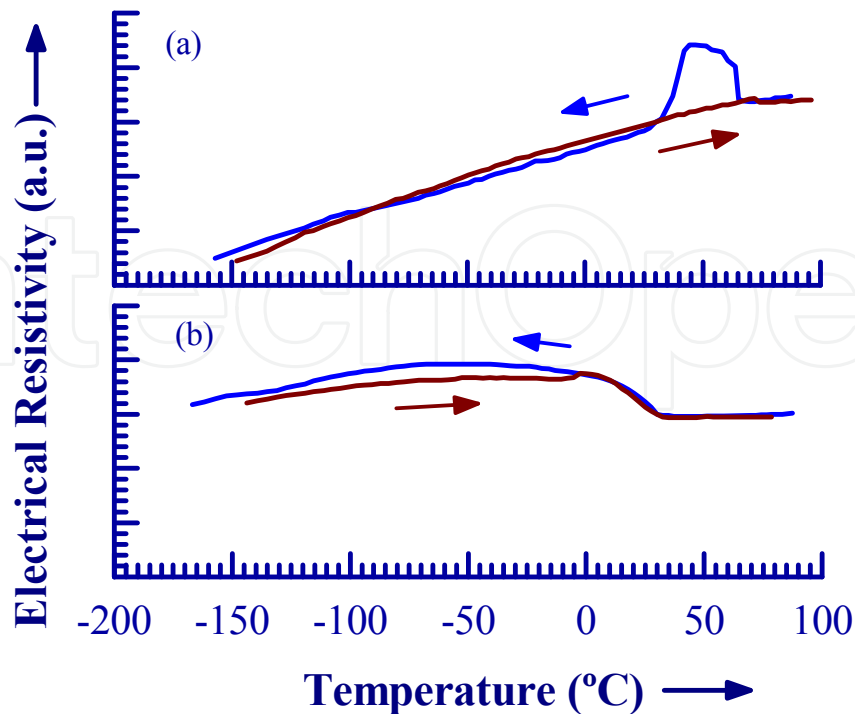
⊕ Multiple-steps with overlap; ∅ suspect multiple-steps with overlap.

**Table 1.** Influence of the thermomechanical processing (marforming) conditions on the transformations sequence.

Deformation up to 10% thickness reduction decreases the shape memory effect capability. This behavior is associated with the reorientation of martensite variants and increase of dislocation density, giving rise to a stabilization of martensite at a higher temperature in agreement with previous results [24].

#### 4. Effect of cooling rate during heat treatments

During the heat treatments, one of the parameters which, can be easily controlled is the cooling rate. Otsuka *et al.*, adopted a heat-treatment in which they homogenized the Ni50at%-Ti alloy for 1 h at 1000 °C followed by furnace cooling to eliminate the vacancies and the disorder to some extent. They found that quenched specimen has almost the same transformation temperatures as the furnace cooled one [25]. It was found earlier by Saburi *et al.*, that during heat-treatment,  $M_s$  and mechanical behavior of Ni-rich off-stoichiometric (>50.7at% Ni) NiTi alloys were sensitive to rate of cooling, whereas, of a near-stoichiometric (50.4 at% Ni) alloys were not [26]. Sitepu *et al.*, showed that precipitation of  $Ni_4Ti_3$  particles occurred in a matrix of Ni-rich Ni-Ti SMA of nominal composition Ni50.7at%-Ti, when it was solution annealed at 850 °C for 15 minutes followed by water quenching and aging at 400 °C for 20 h [27]. In a more recent study, transformation behavior of NiTi alloys of different composition, heat treated by employing quenching and furnace cooling were investigated [28].



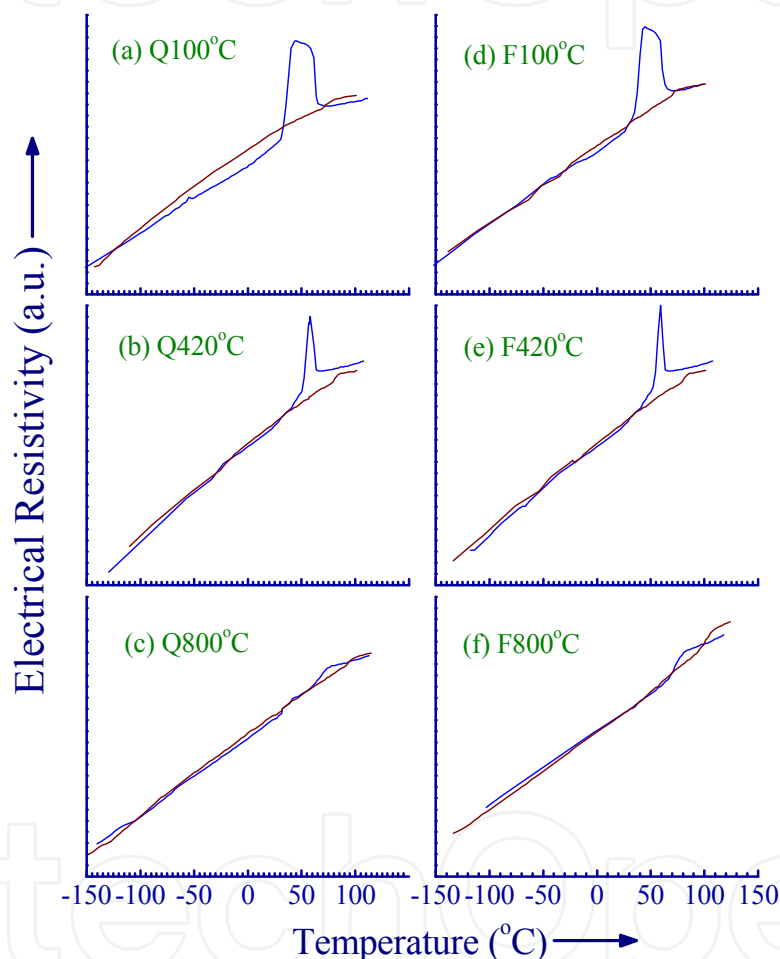
**Figure 5.** Electrical resistivity profiles for (a) Ni54.76wt%-Ti and (b) Ni56.00wt%-Ti alloys in the as-received condition

Fig. 5 shows resistivity profiles for the 2 samples, (a) Ni54.76wt%-Ti, i.e. Ti-rich and Ni56.00wt%-Ti, i.e. Ni-rich Ni-Ti alloys, in the as-received condition. For Ti-rich alloy, R-phase is found to occur only on cooling and the transformation is confined to a temperature interval of about 60°, above 0°C. In the case of Ni-rich alloy, R-phase is found to appear both while heating and cooling, and its temperature interval is spread over a wide temperature range of more than 150°, below +50°C, and these materials do not undergo the transformation to M-phase in the observed temperature range.

Fig. 6 (a-c) and 6 (d-f) show the resistivity profiles of the quenched and furnace cooled samples of Ti-rich alloy, respectively. In both cases, profiles are similar. R-phase transformation is only present during cooling for all the samples annealed between 100° and 420°C and the transformation region decreases, with increase in annealing temperature due to the increase in  $M_s$  temperature. For the annealing temperatures between 420°- 800°C, R-phase is found to be absent.

Fig. 7 (a-d) and 7 (e-h) demonstrate the resistivity profiles of the Ni-rich alloy for the quenched and the furnace cooled samples respectively. For the quenched samples, annealed in the temperature range of 100°- 500°C, two-stage transformation A→R→M during cooling and M→R→A during heating are observed. When annealed between 500° and 600°C, two-stage transformation is observed only in cooling, with decrease in the temperature interval of R-phase. Annealing above 600°C, further suppression of R-phase takes place promoting only M↔A transformation. In the case of furnace cooled alloy, with increase in annealing

temperature, a unique discontinuous behavior is observed. With increase of annealing temperature from 100° to 440°C, two-stage transformation is observed both during cooling and heating in the resistivity profile, with reduced R-phase temperature interval. Annealing the sample between 440° and 580°C, R-phase is found only on cooling with further reduction in the temperature interval. For the sample annealed at 590°C, a sudden increase in the temperature interval of R-phase takes place. Hence, annealing around 590°C seems to be very critical. Annealing above 590°C, two-stage transformation is seen both during heating and cooling in the resistivity profile, regaining the initial behavior. The profiles indicate the stabilization of various phases above annealing temperatures of 590°C.



**Figure 6.** Resistivity profiles for the quenched and furnace cooled Ni<sub>54.76</sub>wt%-Ti alloys annealed at different temperatures.

For lower annealing temperatures, all the samples of the two alloys, both quenched and furnace cooled, exhibit similar behavior, i.e.,  $M_s$  increases with increase in annealing temperature, which is attributed to the release of energy stored during the cold work. Cold work introduces high density of lattice defects, residual strain and internal stresses in the materials, which hinders from the movement of martensite interfaces. On annealing such cold worked materials, thermally activated diffusion leads to the annihilation of lattice defects, promoting martensitic transformation [29]. For the quenched samples, at higher

annealing temperatures, this trend continues and gradual reduction in R-phase facilitates  $M \leftrightarrow A$  transformation. But, the furnace cooled samples, after annealing at higher temperatures, behave differently. A comparison of the resistivity profiles for the quenched and furnace cooled samples, especially annealed at higher temperatures, indicates that Ni-rich alloy is sensitive to the cooling procedure, unlike Ti-rich alloy. There is not much difference in the behavior of Ti-rich alloy either furnace cooled and quenched. In the case of furnace cooled Ni-rich alloy a unique discontinuous behavior is observed, for annealing at 590 °C. This may be due to the microstructural variations, arising as a consequence of two competing processes, viz., annihilation of defects and precipitation. Annealing above this critical temperature, the sample is able to regain and sustain a two-stage transformation, which may be attributed to the dominance of precipitation process over the defect annihilation process. It is proposed that, there is increased chance for  $Ti_3Ni_4$  precipitation while furnace cooling, due to the slow cooling process and the presence of the material at higher temperature for a longer time. As reported by Nishida *et al.*,  $Ti_3Ni_4$  precipitates have rhombohedral structure and are coherent to the matrix having a B2 type structure [30].

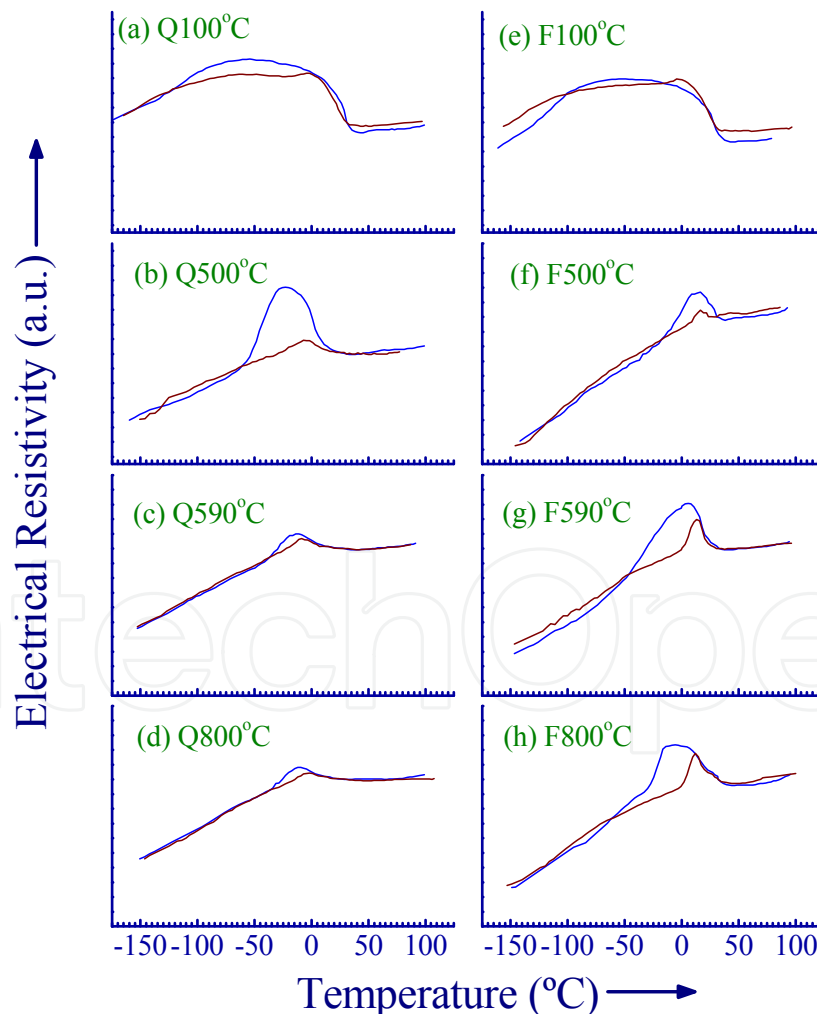


**Figure 7.** Resistivity profiles for the quenched and furnace cooled Ni56wt%-Ti alloys annealed at different temperatures.

## 5. Hot working

Both rolling temperature and thickness reduction are important factors that influence the work hardening and hardness of hot-rolled plates. The greater the thickness reduction, the greater the number of dislocations retained, and therefore, the greater the rate of work hardening. At rolling temperatures  $\geq 600$  °C, recovery or recrystallization occurs. However, because of the short rolling time and the fast cooling in air, the recovery or recrystallization is incomplete [31]. Hot-rolled Ni-Ti materials are found to possess enhanced resistance to low-cycle fatigue (increased pseudoelastic stability) as long as the primary material processing route remains unchanged [32]. Paula *et al.*, recently studied Ni-Ti alloys subjected to heat treatment at 767 °C for 300 s followed by hot rolling (50%) after cooling in air to 500 °C and water quenching to room temperature ( $T_{\text{room}}$ ). Phase transformations were studied using differential scanning calorimetry, electrical resistivity measurements and in situ X-ray diffraction [18].

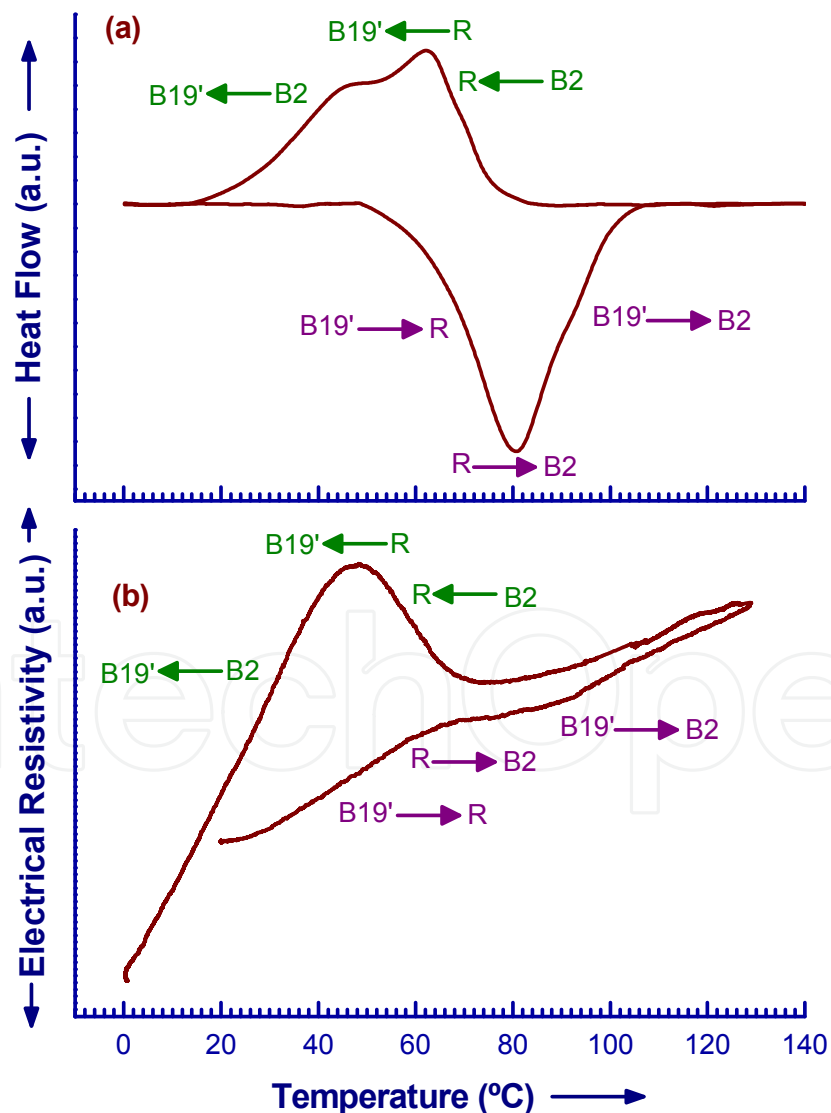


**Figure 8.** (a) DSC and (b) ER curves for TMTHR500 samples.

Fig. 8 (a & b) shows the DSC and ER curves for the ausformed at 500 °C (TMTHR500) samples. During the cooling and heating stages, multiple-step ( $B2 \leftrightarrow R$ ,  $B2 \leftrightarrow B19'$ ,  $R \leftrightarrow B19'$ ) phase transformation is clearly detected in both techniques. During heating, a small kink in the DSC and a small hump in ER plots around 60 °C show the presence of R-phase associated to multiple-step, ( $B19' \rightarrow R$ ,  $B19' \rightarrow B2$ ,  $R \rightarrow B2$ ), phase transformation. It was found that the ausforming at 500 °C promotes multiple-step phase transformation on cooling and heating ( $B2 \leftrightarrow R$ ;  $B2 \leftrightarrow B19'$ ;  $R \leftrightarrow B19'$ ). During the ausforming process at 500 °C, it is not achieved a full recrystallization, in agreement with other authors results [33]. Ausforming introduce many defects in the sample, so that R-phase formation becomes necessary to decrease the energy for  $B2 \rightarrow B19'$  or  $B19' \rightarrow B2$  transformations.

## 6. Thermal cycling

Thermoelastic martensitic transformation appears to be very sensitive to thermal cycling [34, 35]. Also, thermal and mechanical treatments can suppress slip deformation resulting in increase of flow stress and modify the transformation temperatures, recovery stresses and recovery strains [36]. These observations indicate that the transformation process is strongly affected by irreversible changes in the microscopic state of the alloy introduced by thermal cycling. Thermal cycling causes a decrease in the characteristic temperatures and heats of transformation [37]. Also, thermal cycling is found to promote the intermediate R-phase transformation [38]. The effect of training conditions and extended thermal cycling on the two-way shape memory behavior of nitinol has been studied by **Hebda and White, 1995** [39]. Thermal cycling under constant load was studied by **de Araujo et al., 2000** [40] and they concluded that the internal stresses created were effective in inducing two-way memory effect.

Below, in Fig. 9, phase transformations are studied during the ab initio 10 thermal cycles by using DSC and ER techniques. In the DSC, thermal cycle was comprised of heating up to 140 °C, holding for 360 s and subsequently cooling down to -30 °C, with heating and cooling rates being 7.5 K/min. ER characterization have been performed by making use of a home made four-probe setup and the thermal cycling is performed by using the temperature controlled silicone oil bath. Ni-Ti (Ti51at%-Ni) alloy has been previously subjected to a series of thermomechanical treatment followed by heat treatment at 500 °C for 30 min. [41].

In Fig. 9 (a & b), during the first thermal cycle, in both the techniques (DSC & ER), it is observed that one-step phase transformation takes place. As the thermal cycling progresses, phase transformation processes are found to shift toward lower temperatures, both while heating and cooling. In Fig. 9(a), DSC thermograms for the first and second thermal cycles, the phase transformation peaks are observed to be symmetrical both while heating and cooling attributing to one-stage  $M \leftrightarrow A$  transformation. Also, in the ER profile shown in Fig. 9(b) corresponding to the first and second thermal cycles, it is observed that the specimen undergo one-step  $M \leftrightarrow A$  transformation. As the number of thermal cycles is increased, DSC thermogram peaks is found to broaden asymmetrically and shift toward lower temperatures (from the fifth cycle onward), giving rise to increasing evidence of the intermediate R-phase transformation while cooling (Fig. 9b).

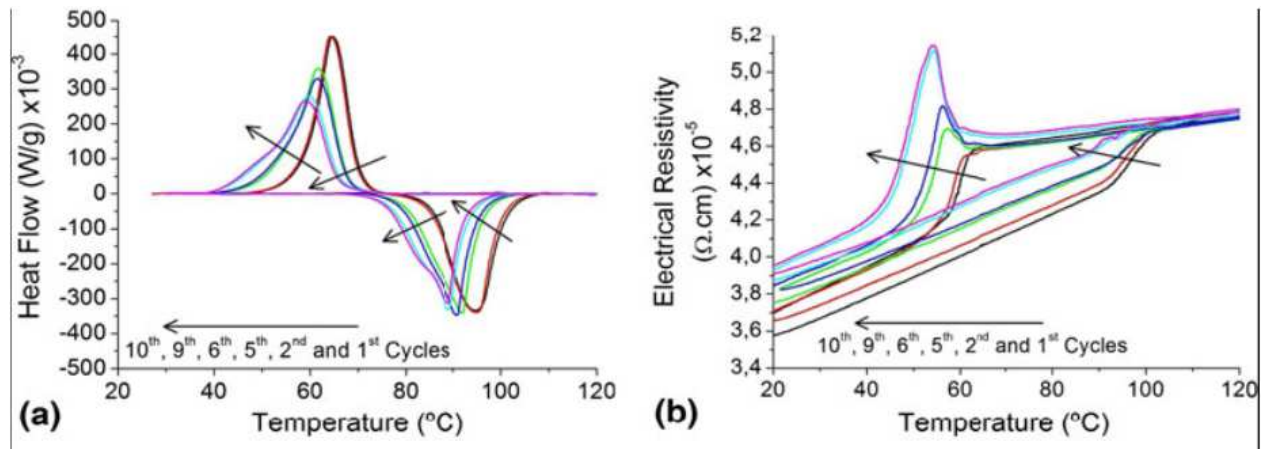


**Figure 9.** Evolution of phase transformation during thermal cycling up to 10 of the Ni-Ti specimens subjected to series of thermomechanical treatment followed by heat treatment at 500 °C for 30 min. (a) DSC and (b) ER profiles.

This shows that the Ti-rich Ni-Ti alloy under study, when subjected to thermal cycling, after multiple steps of thermomechanical treatments followed by final heat treatments, the stability of the phase transformation is found to sensitive and depend on the final heat-treatment temperatures. Further, the thermal cycling process also found to affect the nature of phase transformation. Further, it can also be inferred that different thermomechanical treatments applied on a specimen are found to have opposing effects on the nature of phase transformations. In contrast to the heat treatments, which tend to increase the phase transformation temperatures, thermal cycling tends to decrease them.

## 7. Severe plastic deformation

The plastic deformations carried out by cold-working and hot-working presented above have been extended in the recent past, by subjecting these alloys to severe plastic deformation (SPD). It was shown that the effects of high density of grain boundaries on the martensitic phase transformation and the functional properties of SMA became a focus of research investigating the impact of ultrafine and nanograins on the parameters of the SME and SE. Further, methods of SPD, such as high pressure torsion (HPT) and equal channel angular pressing (ECAP) have been successfully applied to achieve ultrafine grained (UFG) and bulk nanostructured SMA [42–45].

### a. High pressure torsion (HPT)

Waitz et al. [44] showed that martensitic transformation shifts to low temperature when the grain size is less than 150 nm. Initially in their experiments, Ni-Ti alloy was subjected to HPT and later annealed close to recrystallization temperature. By post-deformation annealing at 300°C, it was found that the amorphous structure created by the room-temperature HPT loses its thermomechanical stability and intensively crystallizes [45]. The effect of the composition on the phase transformations in Ni-Ti alloys subjected to HPT and followed by heat treatments was recently reported [46].

Bulk Ni-Ti SMA with different compositions have been chosen and subjected to HPT and their phase transformation characterization was carried out. The selected Ni(49.6 to 49.4at%)-Ti (Ti-rich) alloy in the as-received (AR) condition has  $M_f$  above RT and Ni(around 50.8at%)-Ti (Ni-rich) has  $A_f$  below RT. SPD of Ni-Ti alloys (Ti-rich and Ni-rich) have been performed by HPT at RT. Further, HPT processed separate specimens are subjected to heat treatments at temperatures of 300°C (HPT+HTT300) and 350 °C (HPT+HTT350) for 20 min, and quenched into water at room temperature. Phase transformation temperatures are analyzed by studying the Differential Scanning Calorimeter (DSC) plots. Further, the structural evolution of the samples subjected to SPD in the phase transformation temperature region was studied using in situ X-ray diffraction (XRD) from  $-180$  to  $+180$ °C.

The phase transformation temperatures obtained from the thermogram plots of the corresponding sample conditions are presented in Fig. 10. In Fig. 10a, for the Ti-rich alloy in all the conditions, the transformation temperatures correspond to one-step  $M \leftrightarrow A$  phase transformation both while heating and cooling. While compared to the transformation temperatures of the AR sample, it is observed that, for the HPT sample, there is a slight decrease in  $M_f$  and  $A_s$  temperatures, whereas  $M_s$  and  $A_f$  temperatures increase. As a result, both while heating and cooling, there is a broadening of the temperature intervals in which the phase transformations take place. For the HPT sample after heat treatment at 300°C, designated as HPT+HTT300 in the plot, there is an increase in  $M_f$  and  $A_s$  temperatures, whereas  $M_s$  and  $A_f$  temperatures decrease. These results, both while heating and cooling, on narrowing of the temperature intervals where the phase transformations are taking place. After heat treatment at 350°C, designated as HPT+HTT350 in the plot, all the transformation temperatures increase and the phase transformation temperature intervals become narrower.

In Fig. 10b, for the Ni-rich alloy in the AR and HPT conditions, the transformation characteristics show a one-step  $M \leftrightarrow A$  phase transformation, both while heating and cooling. It is observed that for the HPT sample, the temperatures corresponding to both phase transformations are higher than those corresponding to the AR sample. However, both while heating and cooling, corresponding to  $M \rightarrow A$  and  $A \rightarrow M$  transformations, respectively, there is a narrowing of the transformation temperature intervals. For HPT+HTT300 sample,  $M_s$  decreases,  $A_s$ , and  $A_f$  increase considerably.  $M_f$  decreases to a value below the lower limit of the scanned temperature range. The dashed lines represent the trend of the variation of  $M_f$ . Further, R-phase transformations are present both while heating and cooling. On heat treatment at 350°C after the HPT processing, i.e., for Ni-rich HPT+HTT350, it is observed that all the transformation temperatures tend to increase.

AR samples and samples subjected to HPT of both alloys are scanned using XRD technique at different temperatures in the phase transformation temperature range. 3D view of the XRD profiles obtained while cooling and heating are presented in Fig. 11. Miller indices of the diffraction peaks emerging from the corresponding planes of the phases are marked on each peak. In Fig. 11a, for the Ti-rich Ni-Ti AR sample, it might be observed that the recording of the XRD pattern is started at 180°C, where austenite phase exists, followed by

cooling and recording the spectra at different temperatures until the martensite transformation is complete, i.e., down to  $-40^{\circ}\text{C}$ . Further, the sample is again heated to observe the transformation to austenite, i.e., up to  $180^{\circ}\text{C}$  to complete the thermal cycle. While cooling from  $180^{\circ}\text{C}$  to  $-40^{\circ}\text{C}$ , the peak B2(1 1 0) corresponding to austenite (B2 – cubic structure) gradually disappears and peaks associated to martensite (B19' – monoclinic structure) gradually grow. The diffraction pattern obtained at  $-40^{\circ}\text{C}$ , shows the peaks corresponding to martensite. As the temperature is increased from  $-40$  to  $180^{\circ}\text{C}$ , the peak corresponding to (1 1 0) of austenite (B2 – structure) gradually grows and the peaks corresponding to B19' martensite gradually disappear. In Fig. 11b, for the Ti-rich Ni-Ti sample subjected to HPT, also  $M \leftrightarrow A$  phase transformation behavior is observed.

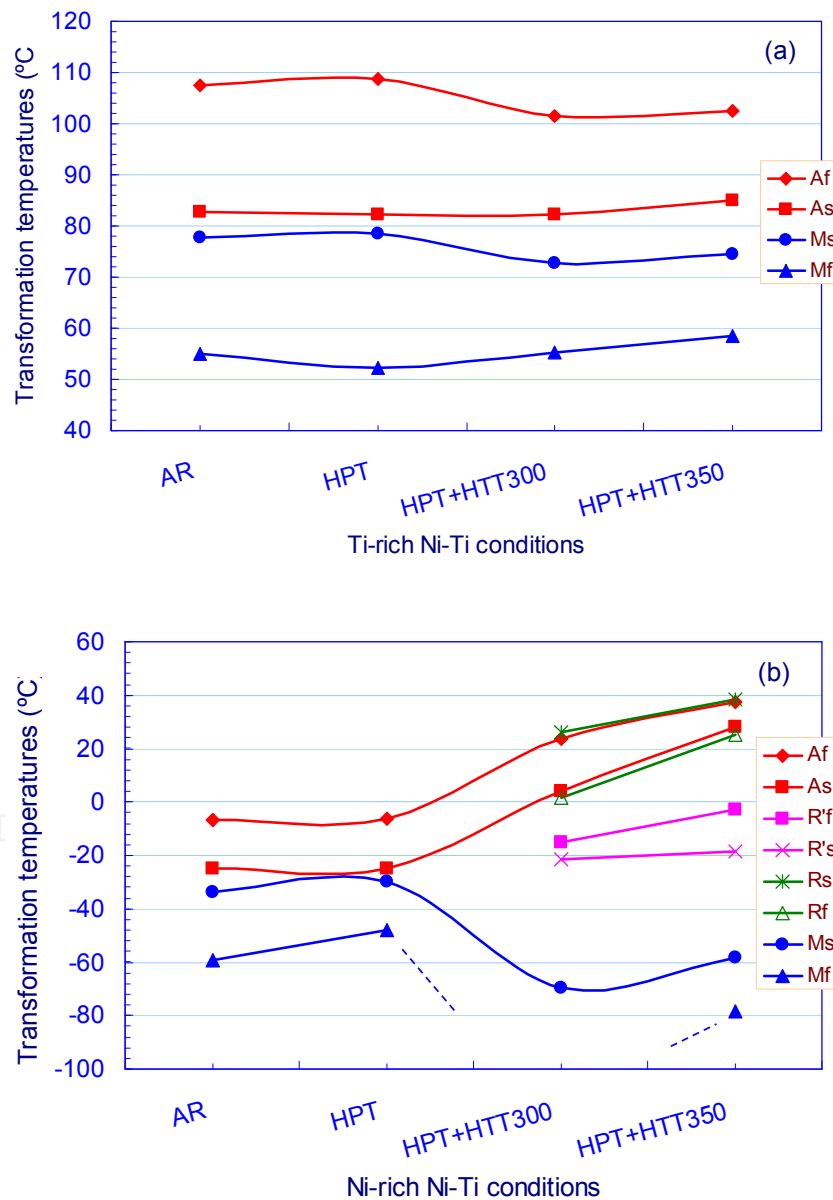


**Figure 10.** Phase transformation temperatures obtained from DSC plots of (a) Ti-rich and (b) Ni-rich Ni-Ti alloys in different conditions.

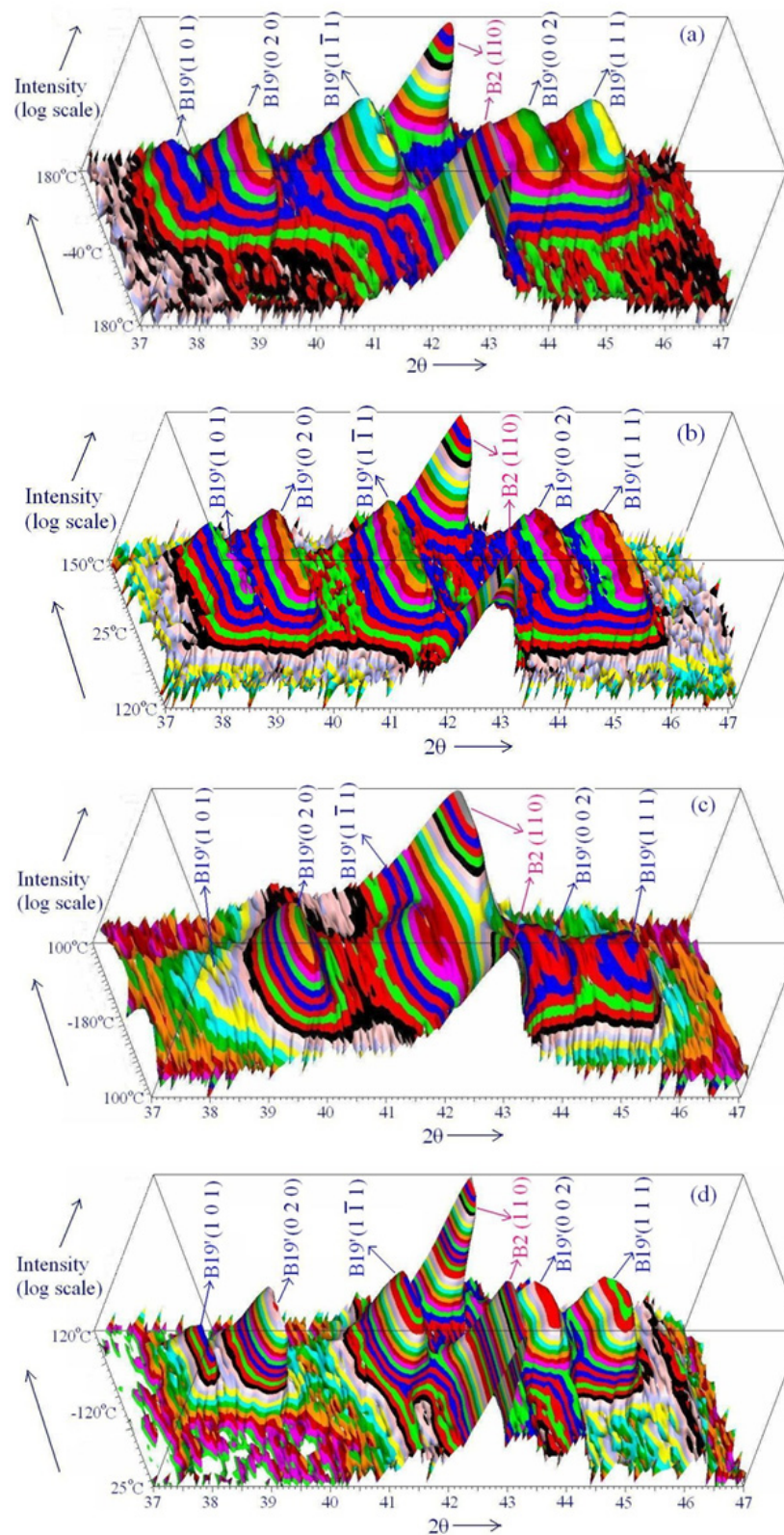


**Figure 11.** 3-D box layout of the XRD profiles obtained during cooling and heating for Ti-rich Ni-Ti alloy in (a) AR and (b) HPT conditions, and Ni-rich Ni-Ti alloy in (c) AR and (d) HPT conditions.

Fig. 11c shows the phase transformation behavior of Ni-rich Ni-Ti alloy in the AR condition. At 100°C, the sample is found to be in austenite (B2) phase. As the temperature is decreased down to -180°C, the intensity of the peak corresponding to B2(1 1 0) decreases. As the cooling progresses, the diffraction peaks corresponding to B19' martensite appear. On heating, the peaks related to B19' martensite disappear and the peak related to B2(1 1 0) appears again. Similar phase transformation behavior is observed for the Ni-rich sample after HPT (Fig. 11(d)). 3D layout of the XRD patterns obtained at selected temperatures during cooling, followed by heating for both Ti-rich and Ni-rich Ni-Ti alloys in HPT+HTT300C and HPT+HTT350C conditions were presented in a recent publication [47]. It is clearly observed that the diffraction peaks corresponding to intermediate R-phase are present for the Ti-rich and absent for the Ni-rich Ni-Ti alloys, both while cooling and heating. The result is in agreement with the transformation temperature profiles obtained by DSC thermogram analyses presented in the above Fig. 10.

The results show that for Ti-rich Ni-Ti alloy, after HPT, as well as following the heat treatments, there are no major changes in the phase transformation behavior. But, for Ni-rich Ni-Ti alloy, there is a slight change in the phase transformation behavior after HPT process, and the final heat treatments bring about very significant change, namely, the presence of intermediate R-phase transformation. In the present experiment, during the HPT process, a high speed of rotation of the piston (1,250 rpm) is involved. Initially, when the pressure torque is applied, a very intense and rapid plastic deformation takes place. This causes the specimen to get macroscopically distorted geometrical shape and eventually microscopic disorder. Owing to the process, the specimen gets heated up and might undergo a short duration annealing in the severely strained condition before cooling to room temperature. This situation may lead to accommodate several conflicting processes [46]. High speed of rotation during the HPT process might also trigger dynamic recrystallization. Depending on factors, such as the previous condition of the HPT specimen, strain accommodated, temperature attained, and magnitude of the time interval at which the specimen is at high temperature, different final microstructural states will be achieved in the specimen. On one hand, the intense deformation will distort the microstructure and long range order will be broken. On the other hand, the high temperature will have its influence on the recovery of the strains and formation of strain free submicrocrystals.

#### **b. Equal channel angular pressing (ECAP) or Equal channel angular Extrusion (ECAE)**

ECAP is an attractive processing technique for several reasons. Processing by ECAP can have a strong effect not only on the mechanical properties but also on the functional properties of materials [48]. However, for Ni-Ti SMA, it is difficult to apply ECAP at RT due to their low deformability and accordingly several reports have appeared describing the fabrication of ultrafine-grained alloys using ECAP at elevated temperatures [49]. The transformation behavior of TiNi alloy after ECAE process has been reported by **Zhenhua Li**

*et al.*, [50] by using the experimental material, Ti-50.6at% Ni alloy rods, with a 25 mm diameter, after 850 °C hot forging and 500 °C annealing for 2 h. They concluded that during high temperature ECAE process, there was no dynamical re-crystallization but, most probably, there was dynamical recovery. Annealed for 5 min at 750 °C after two passes of ECAE, grains were refined and became even. After two passes of ECAE, transformation temperatures of the billet of TiNi alloy sharply decreased. Transformation temperature of the sample remarkably increased annealed for 2 h at 500 °C after two ECAE processes, similar to the one of TiNi alloy before ECAE process, which was related to Ni content in the matrix.

Effect of ECAP process on the microstructure and functional properties, such as recovery stress and maximum fully recoverable strain has been reported. The results show that the multipass ECAP of Ni<sub>50.2</sub>Ti<sub>49.8</sub> alloy allows one to produce a uniform grain structure with predominantly high-angle grain boundaries with a grain size of about 200-300 nm. ECAP increases strength and insignificantly decreases plasticity as compared to the as-quenched state. The strength increases more than 50% with increasing number of passes; after ECAP using 12 passes. The functional properties of the Ni<sub>50.2</sub>Ti<sub>49.8</sub> alloy after ECAP are substantially improved. With increasing number of ECAP passes the maximum recovery stress rises to 1100 MPa and the degree of maximum fully recoverable strain increases to 9.2% [51].

## 8. Concluding remarks

Phase transformations can be studied by using various characterization techniques, such as DSC, ER, Internal Friction (IF), dilatometry, XRD, and optical/electron microscopy [5, 14, 16-19, 41, 43, 52, 53]. Each of these techniques senses different physical phenomena and thus provides information concerning the changes of various physical parameters taking place during the phase transformations. Because of their distinctive nature, when these techniques are employed individually, only partial information about the phase transformation can be delivered.

DSC measures only the sum of all thermal events and, as a result, some important features may be ignored or the results are easily misinterpreted in the cases involving weak and/or complex (overlapping) transformations [5, 16, 18, 19]. ER is the structural sensitive property of a material and it reveals changes during crystallographic phase transformations. In fact, it is found to be more sensitive than DSC in detecting the phase transformations which occur in a narrow temperature range [19, 41]. Dilatometry is capable of sensing small volume changes during phase transformations. Only a limited number of publications report the use of dilatometry to study the phase transformations in Ni-Ti shape memory alloys [17, 19]. These methods have been widely accepted to detect the phase transformations in Ni-Ti SMAs. A combined approach of several characterization techniques would lead to the proper understanding of the phase transformations involved.

## Author details

F.M. Braz Fernandes\* and K.K. Mahesh

*CENIMAT/I3N, Departamento de Ciências dos Materiais, FCT/UNL, 2829-516 Caparica, Portugal*

Andersan dos Santos Paula

*Post-graduated Program in Metallurgical Engineering, UFF - Universidade Federal Fluminense, Volta Redonda, Brazil*

## Acknowledgement

The pluriannual financial support (by Fundação para a Ciência e a Tecnologia – Ministério da Educação e Ciência) of CENIMAT/I3N through the Strategic Project - LA 25 - 2011-2012 and the research project Smart Composites (PTDC/CTM/66380/2006) is gratefully acknowledged by KKM and FMBF. KKM gratefully acknowledges the fellowship under the scheme, 'Ciência 2007' with Ref. No. C2007-443-CENIMAT-6/Ciência2007.

## 9. References

- [1] Effect of Thermal Cycling on the Transformation Temperatures of TiNi Alloys. S. Miyazaki, Y. Igo, K. Otsuka. *Acta Metall.* 34 (1986) 2045–2051.
- [2] Factors Affecting the  $M_s$  Temperature and its Control in Shape-Memory Alloys, K. Otsuka, X. Ren. *Mater. Sci. Forum* 394–395 (2002) 177–184.
- [3] Lattice Transformations Related to Unique Mechanical Effects. J. Perkins. *Metall. Trans.* 4 (1973) 2709–2721.
- [4] Effect of Thermal Cycling on the R-phase and Martensitic Transformations in a Ti-Rich NiTi Alloy. V. Pelosin, A. Riviere, *Metall. Mater. Trans. A* 29 (1998) 1175–1180.
- [5] Effect of Thermal Cycling on R-phase Stability in a NiTi Shape Memory Alloy, J. Uchil, K.G. Kumura, K.K. Mahesh, *Mater. Sci. Eng. A* 332 (2002) 25–28.
- [6] Effect of Deformation and Thermal Treatment of NiTi Alloy on Transition Sequence. Morawiec, D. Stroz, D. Chrobak. *J. Phys. IV* 5 (1995) 205–209.
- [7] Effect of Heat Treatment After Cold Working on the Phase Transformation in TiNi Alloy. T. Todoroki, H. Tamura. *Trans. J. Inst. Met.* 28 (1987) 83–94.
- [8] A study on the wire drawing of TiNi shape memory alloys. S.K. Wu, H.C. Lin, Y.C. Yen. *Materials Science and Engineering A* 215 (1996) 113–119.
- [9] The effects of cold rolling on the martensitic transformation of an equiatomic TiNi alloy. H.C. Lin, S.W. Wu, T.S. Chou, H.P. Kao. *Acta Metall. Mater.* 39 (1991) 2069 - 2080.
- [10] Deformation of Martensite in a Polycrystalline Cu-Zn-Al Alloy. K. Adachi, J. Perkins. *Metall. Trans.* 17A (1986) 945-959.

---

\* Corresponding Author

- [11] FEM Simulation of the Martensitic Transformation in NiTi Alloys. S. Zhang, H. Braasch, P.G. McCormick. *J Phys IV France* 7 C5 (1997) 537-542.
- [12] In-situ High Temperature Texture Characterisation in NiTi Shape Memory Alloy Using Synchrotron Radiation. A.S. Paula, K.K. Mahesh, F.M. Braz Fernandes, R.M.S. Martins, A.M.A. Cardoso, N. Schell. *Materials Science Forum* 495-497 (2005) 125-130.
- [13] Textural Modifications during Recovery in Ti-Rich Ni-Ti Shape Memory Alloy Subjected to Low Level of Cold Work Reduction. A.S. Paula, K.K. Mahesh, N. Schell, F.M. Braz Fernandes, *Materials Science Forum* 636-637 (2010) 618-623.
- [14] Study of the textural evolution in Ti-rich NiTi using synchrotron Radiation. A.S. Paula, J.H.P.G. Canejo, K.K. Mahesh, R.J.C. Silva, F.M. Braz Fernandes, R.M.S. Martins, A.M.A. Cardoso, N. Schell. *Nuclear Instruments and Methods in Physics Research Section B: Beam Interactions with Materials and Atoms* 246 (2006) 206-210.
- [15] Restoration Phenomena of Neutron-irradiated Ti-Ni Shape Memory Alloys. T. Hoshiya, F. Takada, Y. Ichihashi. *Materials Science and Engineering A* 130 (1990) 185-191.
- [16] Effect of Heat Treatment after Cold Working on the Phase Transformation in TiNi Alloy, Tsunehiko Todoraki, Hirokazu Tamura, *Transactions of the Japan Institute of Metals* 28(2) (1987) 83-94.
- [17] Thermal expansion in various phases of nitinol using TMA. J.Uchil, K.P.Mohanchandra, K.Ganesh Kumara, K.K.Mahesh, T.P.Murali. *Physica B (UK)* 270 (1999) 289-297.
- [18] Thermomechanical behaviour of Ti-rich NiTi shape memory alloys. A.S. Paula, K.K. Mahesh, C.M.L. dos Santos, F.M. Braz Fernandes, C.S. da Costa Viana. *Materials Science and Engineering A (UK)* 481-482, (2008) 146-150.
- [19] One- and Two-step Phase Transformation in Ti-rich NiTi Shape Memory Alloy. A.S. Paula, K.K. Mahesh, C.M.L. dos Santos, J.P.H.G. Canejo, F.M. Braz Fernandes. *International Journal of Applied Electromagnetics and Mechanics (Netherlands)* 23 (2006) 25-32.
- [20] Microstructural evolution kinetics after plastic deformation of equiatomic Ti-Ni alloy during isothermal annealings. F. Khelfaoui, G. Thollet, G. Guenin. *Mat. Sci. and Eng. A*, 338 (2002) 305-312.
- [21] Influence of Work Hardening and Heat Treatment on the Substructure and Deformation Behaviour of TiNi Shape Memory Alloys. P. Filip, K. Mazanec. *Scr. Met. et Mat.* 32 (1995) 1375-1380.
- [22] On the  $Ti_2Ni$  precipitates and Guinier-Preston zones in Ti-rich Ti-Ni thin films. J.X. Zhang, M. Sato, A. Ishida. *Acta Mater.* 51 (2003) 3121-3130.
- [23] High-resolution electron microscopy studies on coherent plate precipitates and nanocrystals formed by low-temperature heat treatments of amorphous Ti-rich Ti-Ni thin films. T. Kikuchi, K. Ogawa, S. Kajiwara, T. Matsunaga, S. Miyazaki, Y. Tomota. *Philos. Mag. A* 78 (1998) 467-489.

- [24] Tratamentos Termomecânicos de Ligas do Sistema Ni-Ti. A.S. Paula, Ph.D. Thesis, FCT/UNL, Lisbon – Portugal, 2006.
- [25] Experimental test for a possible isothermal martensitic transformation in a Ti–Ni alloy. K. Otsuka, X. Ren, T. Takeda, *Scripta Materialia* (45)2 (2001) 145–152.
- [26] Effects of Heat Treatment on Mechanical Behaviour of Ti-Ni Alloys. T. Saburi, T. Tatsumi, S. Nenno. *Journal de Physique Colloques* 43(C4) (December 1982) Proceedings of the International Conference on Martensitic Transformations (ICOMAT-82) 261-266.
- [27] Neutron diffraction phase analysis during thermal cycling of a Ni-rich NiTi shape memory alloy using the Rietveld method. H. Sitepu, W.W. Schmahl, J. Khalil Allafi, G. Eggeler, A. Dlouhy, D.M. Tobbens, M. Tovar. *Scripta Materialia*, 46 (2002) 543-548.
- [28] Effect of cooling process during heat treatment on martensitic transformation in Ni-Ti and Ni-Ti-Cr alloys. J. Uchil, K. Ganesh Kumara, K.K. Mahesh. Proc. International Conference on Martensitic Transformations (ICOMAT'02) Helsinki University of Technology, Espoo, Dipoli, Finland, June 10-14, 2002, Edited by J. Pietikainen, O. Soderberg, *J de Physique - IV, France* 112 (2003) 747-750.
- [29] Some aspects of the properties of NiTi shape memory alloy. Y. Liu, J. Van Humbeeck, R. Stalmans, L. Delaey. *Journal of Alloys and Compounds* 247(1997) 115–121.
- [30] Precipitation Processes in Near-Equiatomic TiNi Shape Memory Alloys. M. Nishida, C.M. Wayman, T. Honma. *Metallurgical Transactions A* 17 (1986) 1505-1515.
- [31] Effects of hot rolling on the martensitic transformation of an Equiatomic Ti-Ni alloy. H.C. Lin, S.K. We, *Mater. Sci. Eng. A*158 (1992) 87-91.
- [32] Effect of microstructure on the fatigue of hot-rolled and cold-drawn NiTi shape memory alloys. K. Gall, J. Tyber, G. Wilkesanders, S. W. Robertson, R. O. Ritchie, H. J. Maier. *Materials Science and Engineering A* 486 (2008) 389–403.
- [33] Microstructure and Thermo-Mechanical properties of NiTi shape memory alloys. E. Hornbogen. *Mat. Sci. Forum* 455-456 (2004) 335-341.
- [34] Appearance of an Intermediate Phase with Thermal Cycling on the Transformation of NiTi. H. Matsumoto. *J. Mat. Sci. Letts.* 10 (1991) 408-410.
- [35] Transformation Behavior of NiTi in Relation to Thermal Cycling and Deformation. H. Matsumoto. *Physica B*190 (1993) 115-120.
- [36] P. Filip, K. Mazanec. Influence of Cycling on the Reversible Martensitic-Transformation and Shape-Memory Phenomena in TiNi Alloys. *Scripta Metallurgica et Materialia* 30 (1994) 67-72.
- [37] Kwarciak J., Lekston Z., Morawiec H., Effect of Thermal Cycling and Ti<sub>2</sub>Ni Precipitation on the Stability of the Ni-Ti Alloys. *J. Mat. Sci.* 22 (1987) 2341-2345.
- [38] G. Airoldi, B. Rivolta, C. Turco, Heats of Transformations as a Function of Thermal Cycling in NiTi Alloys, in Proc. Int. Conf. of Martensitic Transformations, JIM Ed., 1986, 691-696.
- [39] D.A. Hebda, S. R. White. Effect of training conditions and extended thermal cycling on nitinol two-way shape memory behaviour. *Smart Mater. Struct.* 4 (1995) 298-304.

- [40] C.J. de Araujo, M. Morin, G. Guenin. Estimation of internal stresses in shape memory wires during thermal cycling under constant load: A macromechanical approach. *J. Int. Mat. Sys. & Structs.* 11 (2000) 516-524.
- [41] A.S. Paula, K.K. Mahesh, F.M. Braz Fernandes, Stability in Phase Transformation after Multiple Steps of Marforming in Ti-rich Ni-Ti Shape Memory Alloy. *Journal of Materials Engineering and Performance*, 20 (2011) 771-775.
- [42] M. Zehetbauer, R. Grossinger, H. Krenn, M. Krystian, R. Pippan, P. Rogl, T. Waitz, R. Wurschum. Bulk Nanostructured Functional Materials By Severe Plastic Deformation. *Adv Eng Mater* 12 (2010) 692-700.
- [43] K.K. Mahesh, F.M. Braz Fernandes, R.J.C. Silva, G. Gurau. Phase transformation and structural study on the SPD NiTi alloys. *Physics Procedia*, 10 (2010) 22-27.
- [44] T. Waitz, V. Kazykhanov, H.P. Karnthaler. Martensitic phase transformations in nanocrystalline NiTi studied by TEM. *Acta Mat* 52 (2004) 137-147.
- [45] Alloy composition, deformation temperature, pressure and post-deformation annealing effects in severely deformed Ti-Ni based shape memory alloys. S.D. Prokoshkin, i.Yu. Khmelevskaya, S.V. Dobatkin, I.B. Trubitsyna, E.V. Tatyandin, V.V. Stolyarov, E.A. Prokofiev *Acta Mater* 53 (2005) 2703-2714.
- [46] K.K. Mahesh, F.M. Braz Fernandes, G. Gurau. Stability of thermal induced phase transformations in the severely deformed equiatomic Ni-Ti alloys. *J Mater Sci* 47(2012) 6005–6014.
- [47] F.M. Braz Fernandes, K.K. Mahesh, R.J.C. Silva, C. Gurau, G. Gurau. XRD study of the transformation characteristics of severely plastic deformed Ni-Ti SMAs. *Phys. Status Solidi C7* (2010) 1348-1350.
- [48] R.Z. Valiev, T.G. Langdon. Principles of equal-channel angular pressing as a processing tool for grain refinement. *Prog Mater Sci* 51 (2006) 881–981.
- [49] V.G. Pushin, R.Z. Valiev The Nanostructured TiNi Shape-Memory Alloys: New Properties and Applications, in *Proceedings of the Symposium on Interfacial Effects in Nanostructured Materials*, Warsaw, Poland, 14-18 September 2002. *Solid State. Phenom.*, 94, (2003) 13–24.
- [50] Z. Li, G. Xiang, X. Cheng. Effects of ECAE process on microstructure and transformation behaviour of TiNi shape memory alloy. *Materials and Design* 27 (2006) 324–328.
- [51] E. Prokofyeva, D. Gunderov, S. Prokoshkin, R. Valiev. Microstructure, mechanical and functional properties of NiTi alloys processed by ECAP technique, in *Proceedings ESOMAT 2009 - 8TH European Symposium on Martensitic Transformations*, Article nr 06028, 5 pgs.
- [52] D. Stroz, Z. Bojarski, J. Ilczuk, Z. Lekston, H. Morawiec. Effect of thermal cycling on as-quenched and aged nickel-rich Ni-Ti alloy. *Journal of Materials Science* 26 (1991) 1741-1748.

- [53] M. Piao, K. Otsuka, S. Miyazaki, H. Horikawa. Mechanism of the  $A_s$  temperature increase by pre-deformation in thermoelastic alloys. *Mater. Trans JIM* 34 (1993) 919–929.

IntechOpen

IntechOpen